Rules of formation of H–C–N–O compounds at high pressure and the fates of planetary ices

Lewis J. Conway[a,b], Chris J. Pickard[c,d], and Andreas Hermann[a,b,1]

[a]Centre for Science at Extreme Conditions, The University of Edinburgh, Edinburgh EH9 3FD, United Kingdom; [b]School of Physics and Astronomy, The University of Edinburgh, Edinburgh EH9 3FD, United Kingdom; [c]Department of Materials Science & Metallurgy, University of Cambridge, Cambridge CB3 0FS, United Kingdom; and [d]Advanced Institute for Materials Research, Tohoku University, Sendai 980-8577, Japan

Edited by Roberto Car, Princeton University, Princeton, NJ, and approved March 25, 2021 (received for review December 22, 2020)

The solar system's outer planets, and many of their moons, are dominated by matter from the H–C–N–O chemical space, based on solar system abundances of hydrogen and the planetary ices H_2O, CH_4, and NH_3. In the planetary interiors, these ices will experience extreme pressure conditions, around 5 Mbar at the Neptune mantle–core boundary, and it is expected that they undergo phase transitions, decompose, and form entirely new compounds. While temperature will dictate the formation of compounds, ground-state density functional theory allows us to probe the chemical effects resulting from pressure alone. These structural developments in turn determine the planets' interior structures, thermal evolution, and magnetic field generation, among others. Despite its importance, the H–C–N–O system has not been surveyed systematically to explore which compounds emerge at high-pressure conditions, and what governs their stability. Here, we report on and analyze an unbiased crystal structure search among H–C–N–O compounds between 1 and 5 Mbar. We demonstrate that simple chemical rules drive stability in this composition space, which explains why the simplest possible quaternary mixture HCNO—isoelectronic to diamond—emerges as a stable compound and discuss dominant decomposition products of planetary ice mixtures.

H–C–N–O chemistry | high pressure | planetary ices | structure search

Crystal structure prediction coupled to electronic structure calculations has emerged as a powerful tool in computational materials science, in particular in the area of high-pressure science, where it can overcome the chemical imagination attuned to ambient conditions: The predictions—and subsequent experimental confirmations—of unusual compounds such as Na_2He, H_3S, or LaH_{10} attest to the predictive power of these approaches (1–6). The planetary ices H_2O, CH_4, and NH_3 may dominate the interiors of icy planets, but under extreme conditions (7–10). High-pressure phases of these ices have been explored computationally, and some predictions of exotic phases of individual ices have also been confirmed by experiments (11–15). Arguably, computational predictions in this field are of crucial importance because of the challenges for laboratory experiments and the indirect nature of astronomical observations. However, with increasing number of constituents the structure searches become computationally much more demanding. Hence, while structure predictions for elemental and binary systems are routine there are far fewer extensive searches of ternary systems, and none for quaternary systems.

The situation in the H–C–N–O quaternary system reflects this. A vast number of publications exist on the high-pressure evolution of the individual constituents H, C, N, and O (16–19). Binary systems have also been looked at in great detail (20–24). The ternary systems are much less investigated: While H–C–O, H–N–O, and C–N–O phase diagrams have been reported (25–27), the H–C–N ternary has not, for example. The PubChem database (28) lists just under 4.8 million molecular H–C–N compounds. Overall, it contains 44.6 million H–C–N–O compounds at ambient pressure, 78% of which are of true quaternary composition—this highlights both the complexity and the relevance of this quaternary system for organic chemistry. Back in the high-pressure area, some binary mixtures of planetary ices, for instance H_2O–NH_3 or N_2–CH_4 mixtures, which form a subset of the H–N–O and H–C–N ternaries, have been studied in simulations into the megabar pressure range (29–32). However, despite the overall importance of H–C–N–O both to planetary science and Earth-bound chemical and life sciences, to our knowledge there are no computational high-pressure studies of this system, or even subsets that include all four elements, for example binary or ternary molecular mixtures such as CO_2–NH_3 or NH_3–H_2O–CH_4. Here, we explore the full H–C–N–O chemical space via crystal structure searches performed at 500 GPa. This resembles the pressure—if not the temperature—at Neptune's core–mantle boundary and therefore helps illuminate potential pressure-induced chemical reactions in the deep interiors of the outer planets and giant icy exoplanets. It also helps us understand more generally what rules govern a familiar composition space at highly unfamiliar external conditions.

Results

The quaternary H–C–N–O phase diagram resulting from our searches is shown in Fig. 1*A*, where all possible compounds are represented within or on the surface of a tetrahedron bounded by H, C, N, and O. We find only one truly quaternary compound to be stable, the 1:1:1:1 compound HCNO, at ambient conditions known as cyanic or fulminic acid, which we discuss in detail further below. We also find five stable structures on three of the

Significance

The planetary ices water, methane, and ammonia, deep inside icy planets, are subject to compression work that matches chemical bond energies. Icy mixtures are then free to form entirely new compounds, based on the energy landscape of the H–C–N–O elemental chemical space. Here, we present an exhaustive survey of this quaternary space aimed at exploring pressure-induced chemical changes, based on structure searches at 5 million atm. Led by the simplest possible compound, HCNO, we find that, at this pressure, stable compounds emerge from simple chemical rules of balanced redox reactions and filled electronic shells. They are mostly hydrogen-poor to form high-density materials. Planetary ice mixtures react to form host–guest compounds, long hydrocarbons, and other materials.

Author contributions: C.J.P. and A.H. designed research; L.J.C. and C.J.P. performed research; L.J.C., C.J.P., and A.H. analyzed data; and L.J.C., C.J.P., and A.H. wrote the paper.

The authors declare no competing interest.

This article is a PNAS Direct Submission.

[1]To whom correspondence may be addressed. Email: a.hermann@ed.ac.uk.

This article contains supporting information online at https://www.pnas.org/lookup/suppl/doi:10.1073/pnas.2026360118/-/DCSupplemental.

Published April 30, 2021.

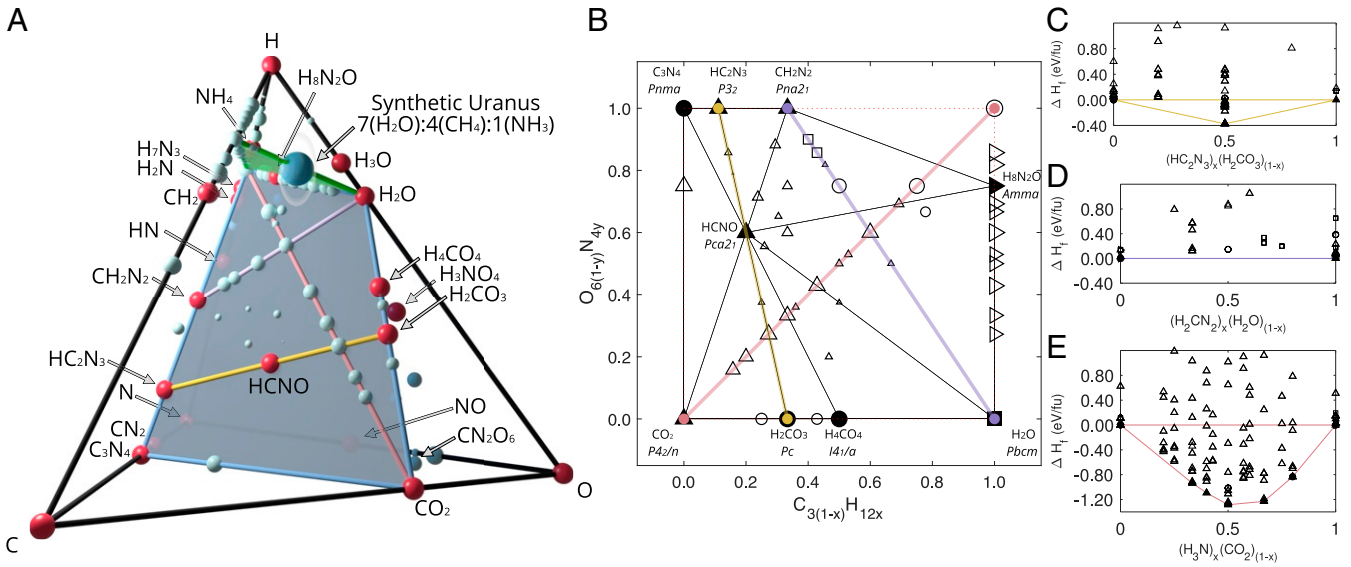

Fig. 1. H–C–N–O phase diagram at 500 GPa from structure searches. (*A*) Full quaternary phase diagram, with the "balanced redox" subspace (see text) shaded in gray and the "planetary ice" triangle H_2O–CH_4–NH_3 in green. Red/blue symbols are stable/metastable phases as labeled; for the latter, size represents closeness to stability, i.e., larger symbols are closer to the convex hull. For reference, the "synthetic Uranus" composition is marked. (*B*) The balanced redox CO_2–C_3N_4–H_2O–NH_3 subspace of H–C–N–O, with select internal one-dimensional cross-sections highlighted. Full/open symbols are stable/metastable phases. Circles/upward triangles/sideways triangles are from searches of the full H–C–N–O space/the CO_2–C_3N_4–H_2O–NH_3 plane/the H_2O–CH_4–NH_3 plane; square symbols are manually added known structures. Larger open symbols are closer to the convex hull. (*C*–*E*) Binary convex hulls from select one-dimensional paths traversing the CO_2–C_3N_4–H_2O–NH_3 plane as shown in *B*; enthalpies are relative to the binary end members which may not be stable in the full quaternary. (*C*) HC_2N_3–H_2CO_3 phases; (*D*) CH_2N_2–H_2O phases; (*E*) CO_2–NH_3 phases.

ternary faces: CH_2N_2 (cyanamide), H_3NO_4 (orthonitric acid), H_8N_2O (ammonia hemihydrate), HC_2N_3 (carbon nitride imide), and CN_2O_6.

Many stable and metastable phases are located on a plane in the three-dimensional composition space that is highlighted in Fig. 1*A* and bounded by CO_2, C_3N_4, H_2O, and NH_3. This plane is drawn up in Fig. 1*B* along the axes CO_2–H_2O and CO_2–C_3N_4. These axes correspond to the conservation of valence electrons along the "transmutation" C $\rightarrow$ 4H and the conservation of electron holes along the "transmutation" 6O $\rightarrow$ 4N, respectively. Compounds in this plane have the formula $C_{3(1-x)}H_{12x}O_{6(1-y)}N_{4y}$ with 12 valence electrons (provided by C/H) and 12 electron holes (provided by O/N). The upper right corner of the plane ($x = 1, y = 1$) is then ammonia, NH_3 (N_4H_{12}) and so on. As a consequence of conserving both electron and hole count, all compounds in this plane are the product of balanced reduction–oxidation (redox) reactions between reducers C and H and oxidizers O and N. Those roles are in line with the electronegativities of these elements at ambient conditions, as well as their estimates at high pressure (33). Moreover, all stable compounds found in this balanced redox plane fulfill the octet rule, where all constituents have filled outer electronic shells. Therefore, a first result from this study is that, even at 500 GPa, most of the stable compounds in the H–C–N–O quaternary (including HCNO) adhere to some of the classic stability criteria for chemical compounds.

Furthermore, most relevant stable or metastable phases within this chemical subspace follow along simple binary mixture lines, which are shown in Fig. 1 *C*–*E*. A straightforward route to create quaternary high-pressure compounds would be from CO_2–NH_3 mixtures. This binary system, shown in Fig. 1*E*, has five mixtures on its convex hull. However, these are all metastable against formation of HCNO, which in turn should be accessible as the 1:1 mixture of CO_2 and CH_2N_2, or HC_2N_3 and H_2CO_3. The situation at lower pressures is discussed further below.

The emergence of the simplest conceivable quaternary compound, HCNO, as a stable point in this quaternary might seem surprising. Fulminic/isocyanic acid, HNCO, was discovered in 1830 by Liebig and Wöhler (34). It usually forms as H–N=C=O or as a tautomer, cyanic acid H–O–C≡N. These are also isomers of fulminic acid, H–C=N–O, which is an explosive. However, HCNO is isoelectronic to diamond, or carbon in general, and in the condensed state might form compact polyhedral networks that lead to stability under pressure. The orthorhombic structure stable at 500 GPa (denoted $Pca2_1$-II) is shown in Fig. 2*B* and appears to be closer to cyanic acid, with buckled graphitic C–N layers connected by C–O bonds to O–H chains. The layers are very close, and carbon is at the center of CON_3 tetrahedra. This structure is stable against decomposition between 240 and 600 GPa; at the low pressure end, it emerges from the HCNO-$Pca2_1$-I structure (see Fig. 2*A* and *SI Appendix*) and at the upper pressure end decomposes into 1/4(C_3N_4 + CH_4O_4). Partial atomic charges based on Bader's topological analysis of the electron density (35) are 0.6, 2.2, −1.6 and −1.2 e for H, C, N, and O, respectively. One can roughly identify these with formal oxidation states +1/+4/−3/−2 and conclude that ionic bonding contributes to HCNO's stability. HCNO is an insulator, with an indirect band gap of 3.73 eV at 500 GPa (see Fig. 2*C*).

HCNO is not only isoelectronic to diamond but also takes up metastable structures that are isostructural with diamond. A monoclinic Pc phase with a cubic diamond topology is very energetically competitive around 250 GPa (see Fig. 2*A*). In fact, this structure can be seen as a quaternary variant of zinc blende (or cubic boron nitride), with alternating sublattices occupied by cations C and H and anions O and N, respectively. Within the H–C–N–O quaternary, the $H_xC_{1-x}N_yO_{1-y}$ subspace contains the compositions that would in theory allow the formation of such quaternary zinc blende structures. The intersection of this subspace with the balanced redox plane is highlighted by the yellow line in Fig. 1 *A* and *B* and gives rise to three stable

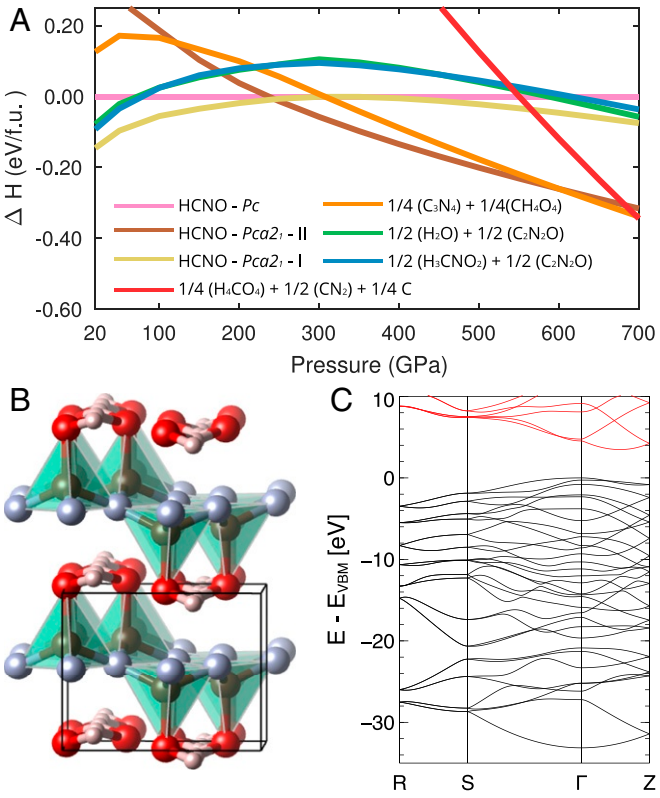

Fig. 2. HCNO at 500 GPa. (*A*) Relative formation enthalpy plot, including all relevant decomposition paths. (*B*) $Pca2_1$-II crystal structure. Pink/brown/gray/red spheres denote H/C/N/O atoms. Unit cell is shown, and CON_3 tetrahedra are highlighted. (*C*) Electronic band structure of HCNO-$Pca2_1$-II.

structures; besides HCNO, these are H_2CO_3, carbonic acid (25), and HC_2N_3, carbon nitride imide.

In total, five stable ternary compounds emerged from the searches at high pressures. The structures of these stable stoichiometries are shown in Fig. 3 (ammonia hemihydrate is discussed in *SI Appendix*). Cyanamide, CH_2N_2, forms a molecular crystal at ambient pressure conditions (36). It can exist as two tautomers: either as the planar molecule N≡C–NH_2 or as H–N=C=N–H, called carbodiimide. The high-pressure structures for CH_2N_2 found here become stable above 10 GPa (see *SI Appendix* for enthalpy data) and are networks structures dominated by C–N covalent bonds and NH$\cdots$N hydrogen bonds. As pressure increases, the N–H$\cdots$N hydrogen bond length decreases and symmetric bridging N–H–N bonds form (see Fig. 3*A*). The partial charges on C/N/H of 2.0/−1.6/0.5 e obtained from a Bader analysis are consistent with formal oxidation states +4/−3/+1 and cyanamide remains an insulator with a band gap of 3.2 eV at 500 GPa. Above 600 GPa CH_2N_2 transforms into a $C2/c$ phase that is isostructural with cubic diamond (see *SI Appendix*), with only the H positions deviating noticeably from tetrahedral sites.

Another stable compound is H_3NO_4 (see Fig. 3*B*). At ambient pressures it can be seen as a nitric acid–water complex, $HNO_3 \cdot H_2O$, which is present in polar stratospheric clouds and forms an ionic structure $(NO_3)^- \cdot (H_3O)^+$ at low temperatures (37). This compound is energetically stable at pressures above 200 GPa (see *SI Appendix*). The structure consists of NO_4 tetrahedra in a body-centered tetragonal arrangement. The terminal oxygen atoms are connected by symmetric buckled O–H–O bonds to form an overall layered structure. The partial charges on the N/O/H atoms are 1.0/−0.8/0.7 e, thus overall slightly less ionic in character than CH_2N_2, in line with relatively close electronegativities of N and O. However, this compound is electronically very stable, with an unusually large band gap of 5.7 eV at 500 GPa.

A third compound, HC_2N_3, is stable accross the pressure range in a $P3_2$ structure similar to hexagonal diamond (see Fig. 3*C*). This is perhaps unsurprising as it has a relatively high carbon content and is isoelectronic to diamond. In fact, this compound has been reported in high-pressure/high-temperature syntheses in a "defective wurtzite" structure (38, 39). The $P3_2$ structure is more stable than the $Cmc2_1$ structure reported in refs. 38 and 39 above 209 GPa (see *SI Appendix*). The partial charges on C/N/H are 2.0/−1.5/0.6 e, very similar to CH_2N_2, and the compound has a band gap of 4.0 eV at 500 GPa.

The slightly more unusual hydrogen-free CN_2O_6 is predicted to be stable above 600 GPa (see Fig. 3*D* and *SI Appendix*). It is the only new stable compound not in the balanced redox subspace. Its structure has a trigonal unit cell dominated by CO_6 octahedra connected by bridging nitrogen atoms such that they form layers in the *ab* plane. Notably, this compound exhibits long-sought-after octahedral coordination of carbon, at significantly lower pressures than in CO_2, where it is predicted to occur at 1,000 GPa (40). The partial charges of the C/N/O atoms are 2.2/0.9/−0.7 e but ionicity is only part of the story, as this is a metallic compound. CN_2O_6 is two electrons short of a filled electronic shell; we constructed quaternary compounds (Be,Mg)CN_2O_6 by placing Be/Mg atoms between the layers of CN_2O_6. These compounds are stable against decomposition and insulating with band gaps of 4.91 and 2.91 eV respectively (see *SI Appendix*).

The stable ternary or quaternary H–C–N–O stoichiometries discussed above are all relatively hydrogen-poor. Amongst previously reported compounds, orthocarbonic acid, H_4CO_4 (25), and ammonia hemihydrate (AHH), H_8N_2O (30), stand out as the most hydrogen-rich ternary phases with 44 and 73 at. % (5 and 15 wt %) hydrogen, respectively. Potential ternary or quaternary phases need to compete with obvious thermodynamic sinks such as carbon dioxide, water, or polyethylene (CH_2), which all benefit from strong covalent and/or ionic bonding. Hence, a second general result from this study is that at 5 Mbar stable (new) structures tend to form covalently bonded polyhedral networks; they require a significant amount of the heavy elements to achieve this: C and N as polyhedra formers, and O (or N) as terminal atoms; their hydrogen content is then relatively low. These network structures are very compact, which favors their formation under pressure, and they tend to feature significant partial charge transfer, resulting in ionic bonding and (with exception of CN_2O_6) insulating character. Fig. 4 shows the chemical bonding as analyzed in real space [via the electron localization function, ELF (41, 42)] and in reciprocal space [via the crystal orbital Hamilton population, COHP (43, 44)]. The ELF shows that all stable structures have strong covalent bonds between the heavy atoms and filled electronic shells around O and N anions. The COHP corroborates that almost all interactions are bonding, with significant individual strength, including O–H and N–H bonds where hydrogen is present: The integrated COHPs up to the respective valence band maxima for the compounds shown in Fig. 4 are in the ranges 5.9 to 6.7 eV for all H–X bonds and 14.2 to 17.6 eV for all heavy element bonds (the C–O bond for octahedrally coordinated carbon in CN_2O_6 is an exception and integrates to 10.3 eV). Only CN_2O_6 and HCNO have some small antibonding character around the Fermi energy and valence band maximum, respectively.

Mixtures of the planetary ices H_2O–CH_4–NH_3 form part of the H–C–N–O quaternary chemical system. However, the only stable compounds in this "planetary ice triangle"' at 500 GPa are H_2O and AHH, whereas CH_4 and NH_3 are unstable

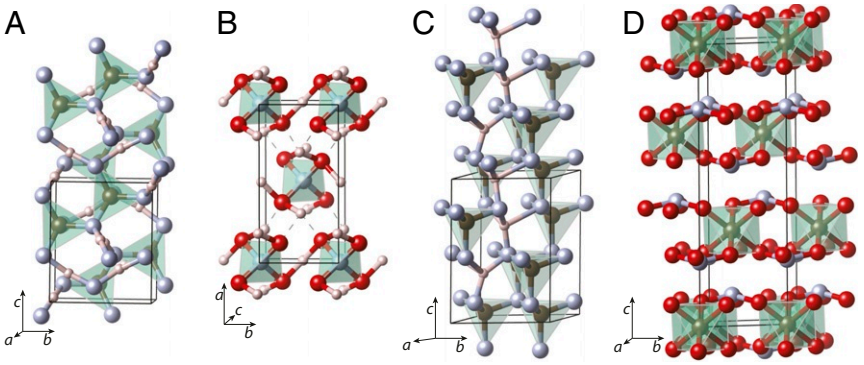

Fig. 3. Crystal structures of stable ternary H–C–N–O phases, with C/N coordination highlighted as appropriate. (*A*) CH_2N_2 (with CN_4 tetrahedra). (*B*) H_3NO_4 (with NO_4 tetrahedra). (*C*) HC_2N_3 (with CN_4 tetrahedra). (*D*) CN_2O_6 (with CO_6 octahedra).

against decomposition into CH_2 plus H_2 and NH_4 plus N_3H_7, respectively. The initial searches did not produce anything—regardless of stability—on the interior of this triangle. Targeted searches of this plane revealed a previously unseen phase of AHH. The structure is more stable than those found in previous searches (31) and extends the maximum stability of AHH from 500 GPa to upward of 800 GPa; see *SI Appendix* for more details. The only stable compound with additional hydrogen is H_3O, where we confirm a recently reported structure (45). The predicted fate of complex icy mixtures depends on composition: A 1:1:1 mixture of H_2O:CH_4:NH_3 is predicted to decompose into H_3O:CH_2:NH_4, with $\Delta H_f = 0.33$ eV/molecule, while a "synthetic Uranus" mixture of solar composition ratio 7:4:1 is slightly less unstable, with $\Delta H_f = 0.25$ eV/molecule against the preferred decomposition into 7^*H_3O:4^*CH_2:NH_4 (both at 500 GPa). Neither case involves the formation of free hydrogen (which could be balanced by formation of some of the stable compounds rich in heavy elements we find here) or free carbon (as diamond). However, small deviations in composition change this; as Fig. 5 shows, a multitude of decomposition pathways exist in the ice plane. Note that formation of diamond and hydrogen are mutually exclusive; the former only appears if the methane molecular ratio is less than 1/3, the latter only if it is larger than 1/3. A third result from this extensive search is therefore that realistic molecular mixtures for icy planet interiors do not always decompose into a hydrogen-rich and a heavy atom-rich component; the "diamond rain"' predicted from the decomposition of methane into diamond and hydrogen (46) is strongly composition-dependent based on ground-state energetics alone. Seen as part of the full H–C–N–O quaternary, this process might not always be relevant. The predicted formation of polyethylene, CH_2, from methane, releases hydrogen but, around the solar composition ratio, much of this would be absorbed into H_3O and NH_4, both of which are host–guest compounds where molecular H_2 is stored in H_2O and NH_3 host matrices, respectively (22, 45). Dynamic compression experiments of polyethylene revealed it to be much more resistant to diamond formation at planetary conditions than, for example, polystyrene, CH (47, 48). Nonetheless, it is likely to be supported by entropy contributions and finite temperature effects: Quasi-harmonic free energy calculations showed that pressures for diamond formation from methane should be much lower at high temperatures (12, 24, 49). More studies are needed on whether this also holds for more complex molecular mixtures.

SI Appendix details outcomes from the structure searches at 500 GPa for all ternary and binary systems and com-

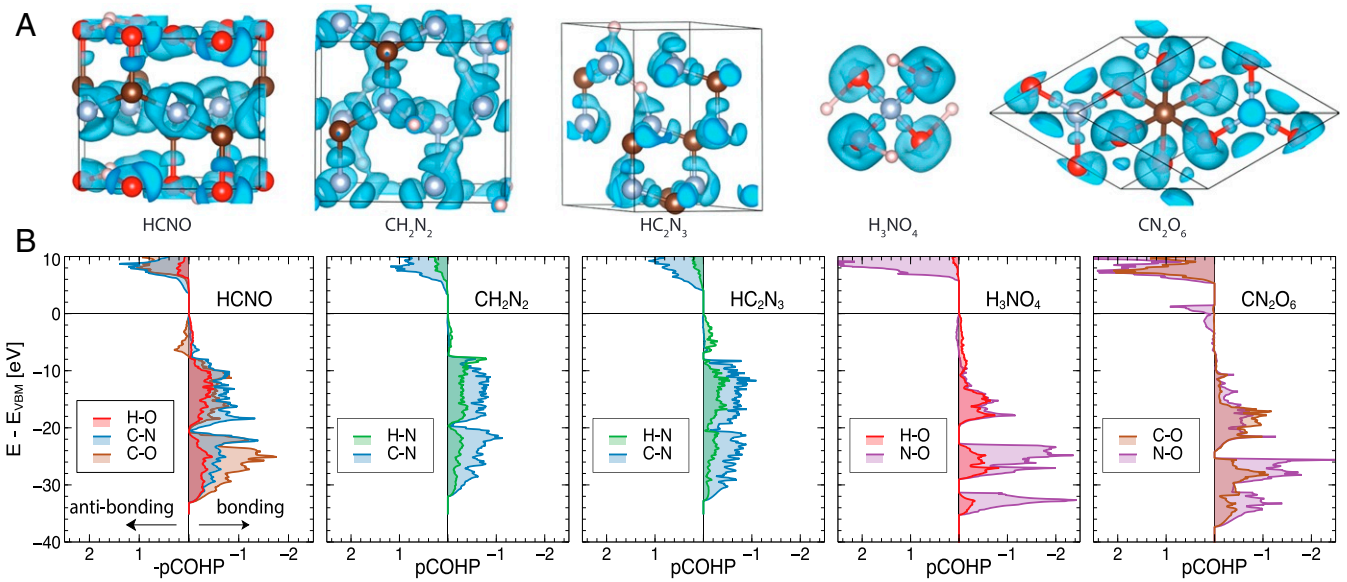

Fig. 4. Chemical bonding analyses. (*A*) Electron localization function isosurfaces (ELF = 0.80) for stable H–C–N–O phases at 500 GPa, all drawn to the same scale. (*B*) COHP analysis for the same structures, projected onto different bond types as indicated.

pares to literature data. In addition, it discusses the H–C–N ternary in more detail that has not yet been covered in the literature.

Our search was targeted at 500 GPa as a typical pressure deep inside Neptune-like planets. Less-extreme conditions are also present and also more easily accessible in experiments. A feature implemented in AIRSS and introduced in ref. 50 allows for a simple linear extrapolation of enthalpy changes, $\Delta H \approx \Delta p \cdot V_0$. This has been used successfully on a variety of high-pressure systems (51) and employed here to generate competitive structures at pressures $p = p_0 + \Delta p$, based purely on search results at $p_0 = 500$ GPa. This method succeeded in finding lower pressure isomers of HCNO and CH_2N_2. We then fully relaxed all potentially interesting structures over a wide pressure range to monitor structural changes and phase transitions and establish lower bounds of stability. In addition, we augmented the dataset by known compounds relevant at lower pressures. While our dataset might not contain all stable structures at lower pressures this analysis should still give an indication of how the H–C–N–O system evolves below 5 Mbar. For instance, the compound HCNO is found to be stable down to at least 20 GPa.

In Fig. 6 we show the "balanced redox" plane spanned by CO_2, H_2O, NH_3, and C_3N_4 at 100 GPa. As at 500 GPa, this plane contains most stable or metastable ternary and quaternary phases. Along the edges, we find stable carbonic acid, H_2CO_3, ammonia hemihydrate $(NH_3)_2(H_2O)$ and quarterhydrate $(NH_3)_4(H_2O)$, cyanamide, CH_2N_2, carbon nitride imide, HC_2N_3, and oxycyanide, C_2N_2O, in agreement with literature (25, 27, 31). All are simple binary mixtures of the end members of this chemical subspace, forming in 1:1, 1:2, or 1:4 ratios. The low-pressure HCNO-$Pca2_1$-I structure remains stable at this pressure and down to at least 20 GPa (see *SI Appendix*) and remains the only stable truly quaternary compound.

Note that the CO_2–NH_3 binary system (pink line in Fig. 6) features a total of seven phases on its convex hull at 100 GPa (see *SI Appendix* for details). However, they are metastable within the full H–C–N–O quaternary system because of the presence of HCNO. For instance, the 1:1 mixture CH_3NO_2 known as nitromethane, is a widely used solvent and fuel additive at ambient conditions and lies just 10 meV/atom away from the hull at

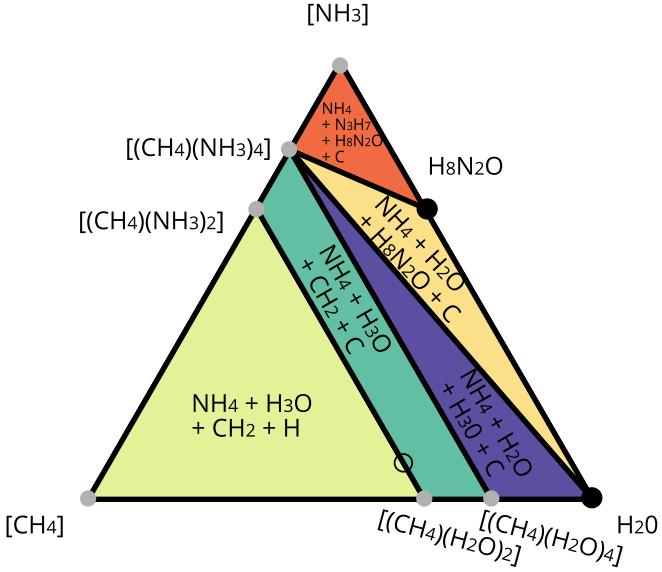

Fig. 5. Ground state phase diagram of the H_2O–CH_4–NH_3 ice plane at 500 GPa. Black (gray) circles denote stable (metastable) phases as labeled, and open circle points to the 7:4:1 solar composition ratio. Regions with different decomposition pathways are colored and labeled.

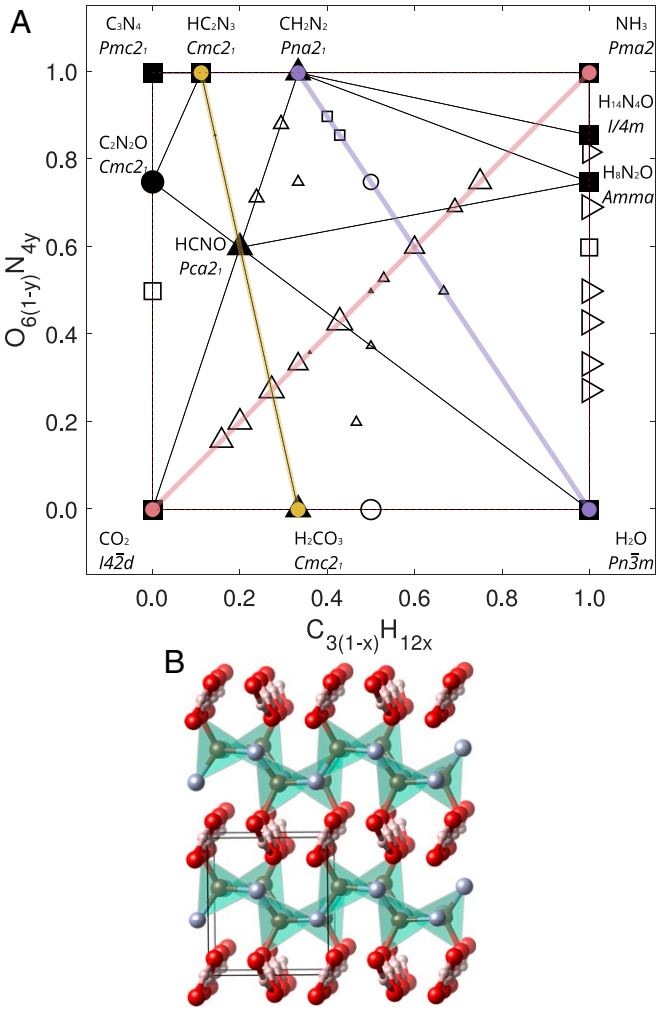

Fig. 6. Calculated H–C–N–O phase diagram at 100 GPa. (*A*) Chemical subspace of "balanced redox"–compliant compounds, drawn to the same specifications as in Fig. 1*B*. (*B*) Crystal structure of HCNO-$Pca2_1$-I at 100 GPa, with unit cell and carbon coordination indicated.

100 GPa. Likewise, the 2:1 mixture, nitroacetic acid $C_2H_3NO_4$, is only 17 meV/atom above the hull. Finally, the 1:2 mixture $CO_2 + 2NH_3$, which forms ionic ammonium carbamate $CO_2(NH_2)^- \cdot (NH_4)^+$ at low temperatures, should decompose into three stable phases (HCNO, water, and ammonia hemihydrate) at 100 GPa but can also be represented as $2H_2O + CH_2N_2$ (purple line in Fig. 6). These CO_2–NH_3 mixtures (or the chemical compounds they form) can thus be used to explore the H–C–N–O quaternary system—all of them should produce HCNO under pressure. Conversely, they could be used to probe the influence of kinetics vs thermodynamics, as kinetic barriers can be significant in reactions of molecular compounds.

The structure of HCNO-$Pca2_1$-I is also shown in Fig. 6. It is similar to HCNO-$Pca2_1$-II at higher pressure, with stronger buckled graphitic C–N layers connected to –(O–H)– chains along the c direction. Partial charges on H/C/N/O of $+0.66/+1.7/-1.15/-1.2$ electrons are also very similar, suggesting similar chemical bonding, while a band gap of 5.5 eV at 100 GPa suggests strong electronic stability.

Discussion

We have reported results from an extensive unbiased structure search of the H–C–N–O chemical space at high pressure, which dominates the interiors of icy planets. Although temper-

ature effects will be crucial in modeling planetary interiors, an understanding of the ground-state pressure-induced chemistry is important in its own right: to explore reactivity and stability in a complex chemical system at extreme conditions from which, for example, detailed pressure-temperature-composition phase diagrams can be constructed subsequently. At pressure conditions that resemble those close to Neptune's core boundary, we find the simplest conceivable quaternary compound, HCNO, to be stable. In addition, we find several other stable ternary compounds, two of which (HC_2N_3 and CH_2N_2) are part of the hitherto unexplored H–C–N ternary system. From our analyses of the distribution of stable structures in chemical space and their chemical bonding we derive various conclusions.

First, most relevant compounds adhere to the octet rule of filled electronic shells and balanced redox reactions, even at 500 GPa. We identify a two-dimensional subspace of H–C–N–O that contains most relevant stable and metastable compounds and is spanned by the transmutations C↔4H and 6O↔4 N, which respectively conserve the number of valence electrons and electron holes. HCNO itself is part of this subspace.

Second, stable compounds of three or four elements are relatively hydrogen-poor. Such compounds can form compact polyhedral networks supported by strong covalent and ionic bonding—which seems to be necessary to retain stability against thermodynamic sinks such as water, carbon dioxide, or polyethylene.

Third, realistic mixtures of planetary ices do not easily decompose into these heavy atom-dominated compounds and either pure hydrogen or carbon (diamond). Around the solar composition ratio, based on ground-state energetics, most hydrogen released when methane forms polyethylene should be absorbed in host–guest networks of the type $(H_2O)_2H_2$ and $(NH_3)_2H_2$. On the other hand, the "diamond rain" of heavy atom material falling through hydrogen-rich matter is, by ground-state energetics, quite composition-dependent: Only methane-poor mixtures (less than 1/3 molecular ratio) result in diamond formation. It remains likely to be facilitated by high temperatures.

At lower pressures, other compounds become relevant, and we suggest using CO_2–NH_3 mixtures as springboard to explore the formation of truly quaternary H–C–N–O compounds in high-pressure environments. An obvious route to explore experimentally is the role of high temperatures: It can change relative free energies, can be used to investigate kinetic barriers toward the formation of the compounds predicted here, and can induce thermal excitations in these compounds (superionicity and melting) that are relevant along typical icy planet isentropes. Looking beyond the H–C–N–O quaternary, the addition of other constituents such as sulfur could be explored; the PubChem database lists 19.8 million molecular compounds in the extended HCNO + S composition space. High pressure leads to different effects there: A C–S–H material was reported to superconduct at room temperature in a high-pressure phases (52), and metallicity and superconductivity is also seen in nitric sulfur hydride N–S–H mixtures (53).

We note that in the process of submitting the current paper, a related manuscript was uploaded to arXiv (54) that supports the stability of HCNO at high pressure.

Materials and Methods

All structure searches were carried out using the AIRSS and CALYPSO codes (50, 55), generating close to 400,000 structures in total. These were acquired in a sequence—all at 500 GPa—that initially searched the entire H–C–N–O quaternary, followed by more targeted searches of several chemical subspaces, with around 280,000 structures in total (56, 57). A further 100,000 structures were generated along the CH_4:NH_3 binary for the range of 4:1 to 1:4 mixtures at 100, 300, and 700 GPa. All of the stable structures reported here, unless otherwise stated, were found by searches of the H–C–N–O quaternary at 500 GPa.

All geometry optimization and phonon calculations were carried out using the CASTEP code (58), the PBE (59) exchange-correlation functional, and ultrasoft pseudopotentials generated on-the-fly by CASTEP. During the searches, geometry optimizations were performed with plane-wave wave cutoff of 340 eV and a k-point spacing of $0.07 \times \pi$Å^{-1}. After screening, a more precise calculation was performed with plane-wave wave cutoff of 1,000 eV and a k-point spacing of $0.04 \times \pi$Å^{-1}.

Precise calculations were carried out on all structures on or close to the five-dimensional convex hull of enthalpy against composition at 500 GPa. To estimate stable structures at lower and higher pressures, members of the two-dimensional convex hull (for each composition) formed of enthalpy against volume were also calculated to a higher precision. Geometry optimizations were performed at pressures between 100 and 700 GPa in increments of 50 GPa. The enthalpies from these calculations were used to determine stable structures. All structures known from the literature which have not been reproduced in this search were manually added to the dataset.

Phonon calculations were carried out on the stable structures to determine their dynamic stability using density functional perturbation theory (60) with norm-conserving pseudo potentials.

Bader charge, ELF, and COHP analyses were performed using wave functions obtained with the VASP code in conjunction with the projector augmented wave method (61, 62) and the PBE exchange-correlation functional (59). Analyses were carried out using the CRITIC2 and LOBSTER packages (63, 64).

Data Availability. Crystal structures and the structure dataset have been deposited in Edinburgh DataShare (https://doi.org/10.7488/ds/3018) and Materials Cloud (https://doi.org/10.24435/materialscloud:p6-zh).

ACKNOWLEDGMENTS. L.J.C. was supported by the Engineering and Physical Sciences Research Council through the Condensed Matter Center for Doctoral Training (EP/L015110/1). C.J.P. was supported by the Royal Society through a Royal Society Wolfson Research Merit award. Computational resources provided by the National Supercomputer Service through the United Kingdom Car-Parrinello Consortium (EP/P022561/1) and project ID d56 "Planetary Interiors" and by the Materials and Molecular Modeling Hub (EP/P020194) are gratefully acknowledged.

1. X. Dong *et al.*, A stable compound of helium and sodium at high pressure. *Nat. Chem.* **9**, 440–445 (2017).
2. D. Duan *et al.*, Pressure-induced decomposition of solid hydrogen sulfide. *Phys. Rev. B Condens. Matter Mater. Phys.* **91**, 180502 (2015).
3. A. P. Drozdov, M. I. Eremets, I. A. Troyan, V. Ksenofontov, S. I. Shylin, Conventional superconductivity at 203 kelvin at high pressures in the sulfur hydride system. *Nature* **525**, 73–76 (2015).
4. F. Peng *et al.*, Hydrogen clathrate structures in rare Earth hydrides at high pressures: Possible route to room-temperature superconductivity. *Phys. Rev. Lett.* **119**, 107001 (2017).
5. Z. M. Geballe *et al.*, Synthesis and stability of lanthanum superhydrides. *Angew. Chem. Int. Ed.* **57**, 688–692 (2018).
6. H. Liu, I. I. Naumov, R. Hoffmann, N. W. Ashcroft, R. J. Hemley, Potential high-Tc superconducting lanthanum and yttrium hydrides at high pressure. *Proc. Natl. Acad. Sci. U.S.A.* **114**, 6990–6995 (2017).
7. W. B. Hubbard *et al.*, Interior structure of Neptune: Comparison with Uranus. *Science* **253**, 648–651 (1991).
8. R. Helled, J. D. Anderson, M. Podolak, G. Schubert, Interior models of Uranus and Neptune. *Astrophys. J.* **726**, 15 (2011).
9. N. Nettelmann *et al.*, Uranus evolution models with simple thermal boundary layers. *Icarus* **275**, 107–116 (2016).
10. R. Helled, N. Nettelmann, T. Guillot, Uranus and Neptune: Origin, evolution and internal structure. *Space Sci. Rev.* **216**, 38 (2020).
11. C. J. Pickard, R. J. Needs, Highly compressed ammonia forms an ionic crystal. *Nat. Mater.* **7**, 775–779 (2008).
12. G. Gao *et al.*, Dissociation of methane under high pressure. *J. Chem. Phys.* **133**, 144508 (2010).
13. A. Hermann, N. W. Ashcroft, R. Hoffmann, High pressure ices. *Proc. Natl. Acad. Sci. U.S.A.* **109**, 745–750 (2012).
14. S. Ninet *et al.*, Experimental and theoretical evidence for an ionic crystal of ammonia at high pressure. *Phys. Rev. B* **89**, 174103 (2014).
15. T. Palasyuk *et al.*, Ammonia as a case study for the spontaneous ionization of a simple hydrogen-bonded compound. *Nat. Commun.* **5**, 3460 (2014).
16. C. J. Pickard, R. J. Needs, Structure of phase III of solid hydrogen. *Nat. Phys.* **3**, 473–476 (2007).
17. J. Sun, M. Martinez-Canales, D. D. Klug, C. J. Pickard, R. J. Needs, Persistence and eventual demise of oxygen molecules at terapascal pressures. *Phys. Rev. Lett.* **108**, 045503 (2012).

18. M. Martinez-Canales, C. J. Pickard, R. J. Needs, Thermodynamically stable phases of carbon at multiterapascal pressures. *Phys. Rev. Lett.* **108**, 045704 (2012).
19. J. Sun, M. Martinez-Canales, D. D. Klug, C. J. Pickard, R. J. Needs, Stable all-nitrogen metallic salt at terapascal pressures. *Phys. Rev. Lett.* **111**, 175502 (2013).
20. D. M. Teter, R. J. Hemley, Low-compressibility carbon nitrides. *Science* **271**, 53–55 (1996).
21. C. J. Pickard, M. Martinez-Canales, R. J. Needs, Decomposition and terapascal phases of water ice. *Phys. Rev. Lett.* **110**, 245701 (2013).
22. G. R. Qian *et al.*, Diverse chemistry of stable hydronitrogens, and implications for planetary and materials sciences. *Sci. Rep.* **6**, 25947 (2016).
23. C. J. Pickard, A. Salamat, M. J. Bojdys, R. J. Needs, P. F. McMillan, Carbon nitride frameworks and dense crystalline polymorphs. *Phys. Rev. B* **94**, 094104 (2016).
24. L. J. Conway, A. Hermann, High pressure hydrocarbons revisited: From van der Waals compounds to diamond. *Geosciences* **9**, 227 (2019).
25. G. Saleh, A. R. Oganov, Novel stable compounds in the C-H-O ternary system at high pressure. *Sci. Rep.* **6**, 32486 (2016).
26. J. Shi, W. Cui, S. Botti, M. A. L. Marques, Nitrogen-hydrogen-oxygen ternary phase diagram: New phases at high pressure from structural prediction. *Phys. Rev. Mater.* **2**, 023604 (2018).
27. B. A. Steele, I. I. Oleynik, Ternary inorganic compounds containing carbon, nitrogen, and oxygen at high pressures. *Inorg. Chem.* **56**, 13321–13328 (2017).
28. S. Kim *et al.*, PubChem 2019 update: Improved access to chemical data. *Nucleic Acids Res.* **47**, D1102–D1109 (2019).
29. M. Bethkenhagen, D. Cebulla, R. Redmer, S. Hamel, Superionic phases of the 1:1 water–ammonia mixture. *J. Phys. Chem. A* **119**, 10582–10588 (2015).
30. V. N. Robinson, Y. Wang, Y. Ma, A. Hermann, Stabilization of ammonia-rich hydrate inside icy planets. *Proc. Natl. Acad. Sci. U.S.A.* **114**, 201706244 (2017).
31. V. N. Robinson, M. Marqués, Y. Wang, Y. Ma, A. Hermann, Novel phases in ammonia-water mixtures under pressure. *J. Chem. Phys.* **149**, 234501 (2018).
32. F. Peng, Y. Ma, A. Hermann, M. Miao, Recoverable high-energy compounds by reacting methane and nitrogen under high pressure. *Phys. Rev. Mater.* **4**, 103610 (2020).
33. M. Rahm, R. Cammi, N. W. Ashcroft, R. Hoffmann, Squeezing all elements in the periodic table: Electron configuration and electronegativity of the atoms under compression. *J. Am. Chem. Soc.* **141**, 10253–10271 (2019).
34. J. Liebig, F. Wöhler, Untersuchungen über die Cyansäure. *Ann. der Phys. und Chemie* **96**, 369–400 (1830).
35. R. F. W. Bader, *Atoms in Molecules: A Quantum Theory* (Oxford University Press, Oxford, 1994).
36. L. Denner, P. Luger, J. Buschmann, X-ray structure of cyanamide at 108 K. *Acta Crystallogr. Sect. C Cryst. Struct. Commun.* **44**, 1979–1981 (1988).
37. R. G. Delaplane, I. Taesler, I. Olovsson, Hydrogen bond studies. XCIII. Oxonium ion in nitric acid monohydrate. *Acta Crystallogr. Sect. B Struct. Crystallogr. Cryst. Chem.* **31**, 1486–1489 (1975).
38. E. Horvath-Bordon *et al.*, High-pressure synthesis of crystalline carbon nitride imide, C_2N_2 (NH). *Angew. Chem. Int. Ed.* **46**, 1476–1480 (2007).
39. A. Salamat *et al.*, Tetrahedrally bonded dense C_2N_3H with a defective wurtzite structure: X-Ray diffraction and Raman scattering re. *Phys. Rev. B* **80**, 104106 (2009).
40. C. Lu, M. Miao, Y. Ma, Structural evolution of carbon dioxide under high pressure. *J. Am. Chem. Soc.* **135**, 14167–14171 (2013).
41. A. D. Becke, K. E. Edgecombe, A simple measure of electron localization in atomic and molecular systems. *J. Chem. Phys.* **92**, 5397–5403 (1990).
42. A. Savin *et al.*, Electron localization in solid-state structures of the elements: The diamond structure. *Angew. Chem. Int. Ed.* **31**, 187–188 (1992).
43. R. Dronskowski, P. E. Blöchl, Crystal orbital Hamilton populations (COHP). Energy-resolved visualization of chemical bonding in solids based on density-functional calculations. *J. Phys. Chem.* **97**, 8617–8624 (1993).
44. S. Maintz, V. L. Deringer, A. L. Tchougréeff, R. Dronskowski, Analytic projection from plane-wave and PAW wavefunctions and application to chemical-bonding analysis in solids. *J. Comput. Chem.* **34**, 2557–2567 (2013).
45. P. Huang *et al.*, Stability of H3O at extreme conditions and implications for the magnetic fields of Uranus and Neptune. *Proc. Natl. Acad. Sci. U.S.A.* **117**, 5638–5643 (2020).
46. M. Ross, The ice layer in Uranus and Neptune—Diamonds in the sky?*Nature* **292**, 435–436 (1981).
47. N. J. Hartley *et al.*, Evidence for crystalline structure in dynamically-compressed polyethylene up to 200 GPa. *Sci. Rep.* **9**, 4196 (2019).
48. D. Kraus *et al.*, Formation of diamonds in laser-compressed hydrocarbons at planetary interior conditions. *Nat. Astron.* **1**, 606–611 (2017).
49. H. Liu, I. I. Naumov, R. J. Hemley, Dense hydrocarbon structures at megabar pressures. *J. Phys. Chem. Lett.* **7**, 4218–4222 (2016).
50. C. J. Pickard, R. J. Needs, Ab initio random structure searching. *J. Phys. Condens. Matter* **23**, 053201 (2011).
51. M. Amsler, V. I. Hegde, S. D. Jacobsen, C. Wolverton, Exploring the high-pressure materials genome. *Phys. Rev. X* **8**, 41021 (2018).
52. E. Snider *et al.*, Room-temperature superconductivity in a carbonaceous sulfur hydride. *Nature* **586**, 373–377 (2020).
53. X. Li, A. Lowe, L. Conway, M. Miao, A. Hermann, Metallic nitric sulfur hydrides under pressure. *Comms. Chem.*, in press.
54. A. S. Naumova, S. V. Lepeshkin, P. V. Bushlanov, A. R. Oganov, Unusual chemistry of the C-H-N-O system under pressure and implications for giant planets. arXiv [Preprint] (2020). https://arxiv.org/abs/2011.12803 (Accessed 22 December 2020).
55. Y. Wang, J. Lv, L. Zhu, Y. Ma, CALYPSO: A method for crystal structure prediction. *Comput. Phys. Commun.* **183**, 2063–2070 (2012).
56. L. J. Conway, C. J. Pickard, A. Hermann, Rules of formation of H–C–N–O compounds at high pressure and the fates of planetary ices. Edinburgh DataShare. https://doi.org/10.7488/ds/3018. Deposited 12 April 2021.
57. L. J. Conway, C. J. Pickard, A. Hermann, Rules of formation of H–C–N–O compounds at high pressure and the fates of planetary ices. Materials Cloud Archive. https://doi.org/10.24435/materialscloud:p6-zh. Deposited 12 April 2021.
58. S. J. Clark *et al.*, First principles methods using CASTEP. *Zeitschrift für Krist. Cryst. Mater.* **220**, 567–570 (2005).
59. J. P. Perdew, K. Burke, M. Ernzerhof, Generalized gradient approximation made simple. *Phys. Rev. Lett.* **77**, 3865–3868 (1996).
60. K. Refson, P. R. Tulip, S. J. Clark, Variational density-functional perturbation theory for dielectrics and lattice dynamics. *Phys. Rev. B* **73**, 155114 (2006).
61. G. Kresse, J. Furthmüller, Efficient iterative schemes for ab initio total-energy calculations using a plane-wave basis set. *Phys. Rev. B* **54**, 11169–11186 (1996).
62. G. Kresse, D. Joubert, From ultrasoft pseudopotentials to the projector augmented-wave method. *Phys. Rev. B* **59**, 1758–1775 (1999).
63. A. Otero-De-La-Roza, E. R. Johnson, V. Luaña, Critic2: A program for real-space analysis of quantum chemical interactions in solids. *Comput. Phys. Commun.* **185**, 1007–1018 (2014).
64. R. Nelson *et al.*, LOBSTER: Local orbital projections, atomic charges, and chemical-bonding analysis from projector-augmented-wave-based density-functional theory. *J. Comput. Chem.* **41**, 1931–1940 (2020).